WORLD CONFERENCE ON TIMBER ENGINEERING 2025
BRISBANE, AUSTRALIA
Advancing Timber for the Future Built Environment

DETERMINATION OF CANADIAN SEISMIC FORCE MODIFICATION FACTORS FOR POST-TENSIONED ROCKING CLT WALLS

Huanru Zhu[1], Matiyas A. Bezabeh[2], Asif Iqbal[3], Marjan Popovski[4], Zhiyong Chen[5]

ABSTRACT: Post-tensioned cross-laminated timber (PT-CLT) rocking walls with energy dissipation devices (EDDs) have proved to be a resilient seismic force-resisting system (SFRS). Previous studies have demonstrated their satisfactory performance in high seismic risk zones in Canada. Nonetheless, challenges remain for this system to be practically adopted due to the absence of SFRS force modification factors (overstrength-related factor, R_o, and ductility-related factor, R_d) in the National Building Code of Canada. This study evaluates R_d and R_o factors for PT-CLT rocking walls with EDDs following an approach released by the National Research Council Canada. An R_o of 1.5 and an R_d of 4 were initially considered. To reflect potential variability in seismic design, 69 archetype buildings were designed. A multi-spring numerical modelling strategy in *OpenSeesPy* was first validated with shaking table tests and then used to model all archetypes. Nonlinear response history analysis was then conducted for each archetype using site-specific ground motions scaled to 100% and 200% design-level earthquakes to evaluate whether a system could satisfy the acceptance criteria outlined in the method. The investigation concluded that an R_o of 1.5 and an R_d of 4 can be used for seismic design of PT-CLT rocking wall buildings in Canada.

KEYWORDS: Cross-laminated timber (CLT); post tensioned system; seismic force modification factor; National Building Code of Canada

1 – INTRODUCTION

Mass timber has become a competitive and promising construction material in North America due to its inherent environmental sustainability and aesthetic appearance [1–2]. Wider adoption of mass-timber construction can help Canada achieve net-zero carbon emissions by 2050, address the housing crisis, and create employment opportunities in rural and Indigenous communities. These needs have resulted in rapid growth of mass-timber construction and advances in building codes. Ductility and energy dissipation in traditional mass-timber buildings depend on metal connectors between wood members. During seismic excitation, permanent damage to connectors can result in significant residual drift of buildings, subsequent high repair costs, and risk of aftershock collapse, as well as the potential need for building demolition. To enhance seismic performance and reduce residual damage, a post-tensioned rocking wall system incorporating mass-timber panels (Pres-Lam walls) and replaceable energy dissipation devices (EDDs) can be employed [3–8] (Fig. 1).

Global efforts have been made to explore the lateral behaviour and seismic performance of Pres-Lam walls using both experimental [3–5] and numerical modelling approaches [6–8]. Recent testing in North America was mostly carried out using post-tensioned cross-laminated timber (PT-CLT) walls. These included reversed quasi-static cyclic tests [3] and full-scale shaking table tests of two-story [4] and ten-story PT-CLT rocking wall buildings [5]. In Canada, Kovacs and Wiebe [6] conducted collapse assessments for PT-CLT rocking wall buildings without EDD in Montreal, a region of moderate seismicity dominated by crustal events. Zhu et al. [7-8] applied a direct displacement-based design approach to design mid- and high-rise PT-CLT rocking wall buildings in Vancouver, a city of high seismicity and complex

[1] Graduate Student, Department of Civil Engineering, McGill University, Montreal, Canada, huanru.zhu@mail.mcgill.ca

[2] Assistant Professor, Department of Civil Engineering, McGill University, Montreal, Canada, matiyas.bezabeh@mcgill.ca

[3] Associate Professor, School of Engineering, University of Northern British Columbia, Prince George, Canada, asif.Iqbal@unbc.ca

[4] Principal Scientist, Building Systems, FPInnovations, Vancouver, Canada, marjan.popovski@fpinnovations.ca

[5] Scientist, Building Systems, FPInnovations, Vancouver, Canada, zhiyong.chen@fpinnovations.ca

https://doi.org/10.52202/080513-0493

seismotectonics in Canada. Their satisfactory seismic performance was demonstrated based on nonlinear dynamic analyses, highlighting the promising applicability of such seismic force resisting system (SFRS). However, challenges remain for practical adoption of this system in Canada due to the absence of SFRS force modification factors (i.e., overstrength-related factor, R_o, and ductility-related factor, R_d) in the latest editions of the National Building Code of Canada (NBCC) [9].

To determine R_d and R_o for newly developed SFRSs, most previous studies followed the procedure outlined in FEMA P695 [10]. However, differences in seismic hazard, performance objectives (POs), building design, and construction practices between Canada and the U.S. limit its direct applicability [11]. These differences create inconsistencies in collapse definitions, ground motion selection, and uncertainty quantification. Another limitation is the mandatory usage of incremental dynamic analysis (IDA), which is typically computationally exhaustive when large numbers of prototype buildings have been designed and are to be assessed.

To address these, the Canadian Construction Materials Centre (CCMC) at the Construction Research Centre at the National Research Council Canada (NRCC-CRC) developed a technical guide offering a simplified procedure to evaluate R_d and R_o factors [12]. The CCMC method enables direct assessment of SFRS seismic performance against the performance objective outlined in NBCC [9]. This refers to a global limit of 2.5% building inter-story drift (ISD) under the design-level earthquake (DLE) (2% in 50 years). Such a limit state is called extensive damage and falls between the POs of life safety (LS) and collapse prevention (CP) for buildings of normal importance (i.e., office or residential); it is different from the structural collapse targeted in FEMA P695 [10]. Moreover, depending on available information related to the SFRS, the CCMC approach provides three methods to select trial R_d factors. It is also suggested that the site-specific ground motion ensemble should be selected and scaled based on NBC Commentary J [9], rather than on the fixed set of ground motions provided by FEMA P695. Furthermore, the CCMC approach assesses the adequacy of the proposed R_d and R_o using nonlinear response history analysis (NLRHA) and does not require IDA. Hence, adopting the CCMC approach can ensure that the development process considers Canadian seismicity, POs, and design requirements while avoiding the computational exhaustiveness of IDA. It is noteworthy that such a method has been applied in a previous study by Yang et al. [2] for an innovative balloon-type CLT building with rocking shear walls.

To facilitate practical adoption of PT-CLT walls as SFRSs in Canada, this study evaluates the R_d and R_o factors for PT-CLT rocking walls with EDDs following the CCMC procedure. An R_o of 1.5 and an R_d of 4 were initially considered. To reflect potential variability in building geometry, system configuration, and seismic hazards, 69 archetype buildings were designed, and a prescriptive approach was adopted in accordance with NBCC [9]. A robust multi-spring numerical modelling strategy in *OpenSeesPy* was first validated with shaking table tests and then used to model all archetype buildings. To validate the R_o factor, nonlinear static analysis was first conducted. Next, based on the CCMC procedure, NLRHA was conducted for each archetype using site-specific ground motions scaled to 100% and 200% DLEs to evaluate whether the system could satisfy the acceptance criteria outlined in the CCMC method.

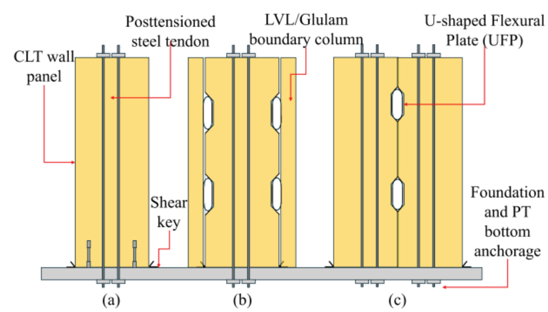

Figure 1. PT-CLT wall configurations: (a) Single wall (SW); (b) Column-wall-column (CWC); (c) Coupled walls (CW).

2 – THE CCMC APPROACH

This section provides an overview of the CCMC approach, and a flowchart outlining the key steps adopted in this study is shown in Fig. 2. Readers can refer to [2, 12] for further details. In Step 1, the required system information is outlined. This includes the load path, the system's structural limit states, and any lateral behaviour. The yielding and capacity-protected elements must also be clearly defined. In Step 2, R_d and R_o should be preliminarily selected based on available information and understanding of the system, which can guide the initial selection based on engineering judgment. Three methods are provided, depending on the level of available SFRS information based on existing analytical, experimental, or numerical studies. With the trial R_d and R_o, archetypes should then be designed following a prescriptive procedure aligning with NBCC. The design may involve an equivalent static force procedure (ESFP) or a modal response spectrum analysis (MRSA). In Step 3, a robust numerical modelling strategy must be developed or

https://doi.org/10.52202/080513-0493

adopted that can explicitly model the yielding mechanism, the yielding elements, and the mass distribution of the system. Simulated or non-simulated collapse mechanisms must also be defined. To conduct NLRHA, in Step 4, site-specific ground motions should be selected based on the requirement prescribed in the NBCC Commentary J [9]. Next, the seismic performance of each designed archetype is assessed with ground motions scaled to 100% DLE. The design is considered as acceptable if less than 10% of the ground motions result in unacceptable structural response (e.g., exceeding the 2.5% global ISD limit, excessive component-level strain or deformation, yielding of capacity-protected elements, or numerical instability). If the performance evaluation at 100% DLE is passed, archetypes are to be further examined with ground motions scaled to 200% DLE in Step 6. If more than 50% of the ground motions result in an unacceptable response, the system is considered to have failed. It is suggested that a 4.5% global ISD limit can be considered at 200% DLE [2, 12]. If all designed archetypes satisfy both acceptance criteria at both levels, the proposed SFRS and its related R_d and R_o factor and design procedure will be sent for peer review and potential adoption. If not, modifications and iterations are needed from Step 2.

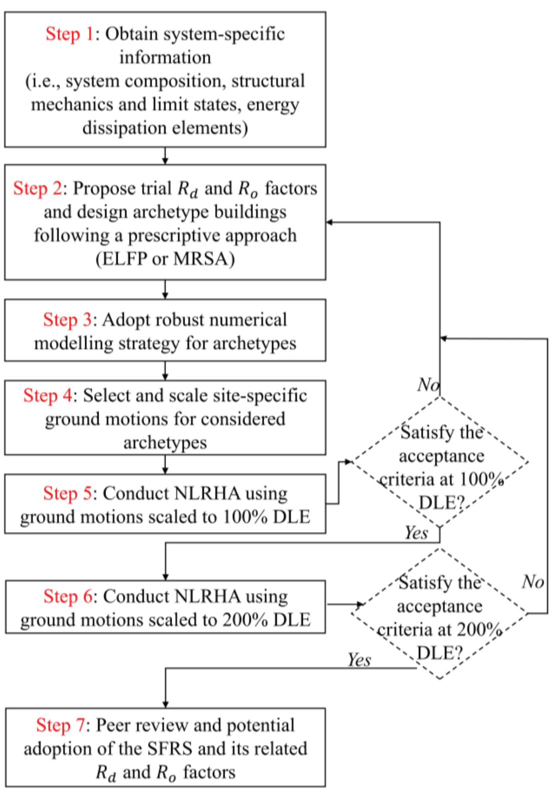

Figure 2. Performance assessment using the CCMC approach

3 – ARCHETYPE BUILDINGS AND SEISMIC DESIGN

3.1 LATERAL BEHAVIOR OF PT-CLT WALL

A PT-CLT wall is made up of vertically stacked CLT panels clamped by unbonded post-tensioned steel tendons from the wall top to the wall-to-foundation interface (Fig. 1). Although a CLT panel can provide in-plane stiffness, PT elements will exert a restoring moment to re-centre the system when elongated under lateral loading. Sliding can be prevented with shear keys. Various types of EDDs can be coupled to the system. This typically includes buckling-restrained axial fuses (BRAFs) [3, 7] and U-shaped flexural plates (UFPs) [3–5]. Under lateral loading, the initial resistance of a PT-CLT wall can be attributed to the initial post-tensioning force and self-weight of the CLT wall, and only panel elastic deformation takes place. With increased loading, base uplift or gap opening of the panel occurs. Due to material and geometric nonlinearities, EDDs can undergo plastic deformation during rocking. Hence, seismic energy input can be effectively dissipated, and primary structural components can be protected by the sacrificial EDDs. The overall building hysteresis, combining both re-centring and energy dissipation, therefore exhibits a flag shape. Based on past studies, three structural PT-CLT wall configurations commonly exist (Fig. 1): (1) SW: a single PT-CLT wall equipped with BRAFs at the wall-to-foundation interface; (2) CWC: a single PT-CLT wall confined by boundary columns on both sides, with UFPs distributed between the wall and the columns; (3) and CW: two PT-CLT walls connected in series, with UFPs serving as the coupling link.

3.2 DEVELOPMENT OF ARCHETYPE BUILDINGS

Archetype buildings with a typical floor plan, as shown in Fig. 3, were developed in this study. Each building has ten PT-CLT walls positioned in the N-S direction. These buildings were designated as normal-occupancy office buildings and were situated on Site Class D soil. For each structural configuration, 23 archetypes, grouped into 10 PGs, were developed. Using the CWC-type PT-CLT rocking wall buildings as an example, the archetypes in PGs 1 to 5 and 6 to 10 were hypothetically designed for Vancouver, British Columbia, and Montreal, Quebec, respectively, to represent seismic categories (SCs) 3 and 4 (moderate and high seismicity), as defined by NBCC [9]. Note that the CCMC approach suggests five representative locations for seismicity on Site Class D soil: Tofino, Victoria, Vancouver, Montreal, and Toronto. However, for simplicity and practical design considerations, only Montreal and Vancouver were selected for this study. The

https://doi.org/10.52202/080513-0493

archetypes in PGs 1 and 6 feature a bottom-floor height of 3.6 m and a typical story height of 3.2 m, ensuring compliance with NBCC height limits for platform-type mass-timber SFRS (i.e., 20 m for SC 4 and 30 m for SC 3).

Table 1. Performance groups and archetype information for CWC-type PT-CLT rocking wall buildings designed with $R_d = 4$.

Archetype	SC	Number of stories	Bottom floor height (m)	Story height (m)	Building height (m)	Re-centring ratio	Floor system
1 (PG 1)	4	3	3.6	3.2	10	0.7	TCCF
2 (PG 1)	4	6	3.6	3.2	19.6	0.7	TCCF
3 (PG 2)	4	3	6	3.5	13	0.7	TCCF
4 (PG 2)	4	3	6	4.2	14.4	0.7	TCCF
5 (PG 3)	4	9	3.6	3.2	29.2	0.7	TCCF
6 (PG 3)	4	6	6	3.5	23.5	0.7	TCCF
7 (PG 4)	4	3	3.6	3.2	10	0.6	TCCF
8 (PG 4)	4	6	3.6	3.2	19.6	0.6	TCCF
9 (PG 5)	4	3	3.6	3.2	10	0.7	CLT
10 (PG 5)	4	6	3.6	3.2	19.6	0.7	CLT
11 (PG 6)	3	3	3.6	3.2	10	0.7	TCCF
12 (PG 6)	3	6	3.6	3.2	19.6	0.7	TCCF
13 (PG 6)	3	9	3.6	3.2	29.2	0.7	TCCF
14 (PG 7)	3	3	6	3.5	13	0.7	TCCF
15 (PG 7)	3	6	6	4.2	27	0.7	TCCF
16 (PG 8)	3	9	6	3.5	34	0.7	TCCF
17 (PG 8)	3	9	6	4.2	39.6	0.7	TCCF
18 (PG 9)	3	3	3.6	3.2	10	0.6	TCCF
19 (PG 9)	3	6	3.6	3.2	19.6	0.6	TCCF
20 (PG 9)	3	9	3.6	3.2	29.2	0.6	TCCF
21 (PG 10)	3	3	3.6	3.2	10	0.7	CLT
22 (PG 10)	3	6	3.6	3.2	19.6	0.7	CLT
23 (PG 10)	3	9	3.6	3.2	29.2	0.7	CLT

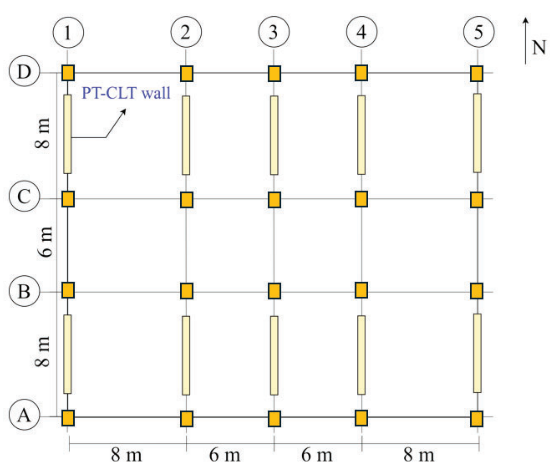

Figure 3. Archetype building floor plan.

To account for potential use of the first story as an office building with commercial spaces, PGs 2 and 7 adopt a 6-m bottom-floor height while still staying within the NBCC height limits. Based on the satisfactory performance observed in a previous shaking-table test of a 10-story PT-CLT shear wall building [4], PGs 3 and 8 explore archetype buildings with heights exceeding the NBCC limit for platform-type buildings. In addition, the design re-centring ratio, which is the ratio of the moment resisted by PT elements to the total moment resistance of the system, is considered as a variable. Although PGs 1–3 and 6–8 use a re-centring ratio of 70%, PGs 4 and 9 adopt a lower ratio of 60%, offering higher energy dissipation. To enhance vibration control, all these PGs use timber-concrete composite floors (TCCF), which results in higher seismic mass. However, PGs 5 and 10 explore an alternative floor system consisting of CLT panels only, which is designed to consider low-gravity load scenarios. Table 1 summarizes the details of the CWC archetype design with $R_d = 4$. Using the same considerations, SW-type and CW-type PT-CLT rocking wall buildings were developed. Hence, 69 archetypes binned into 30 PGs were designed in this study.

3.3 PRESCRIPTIVE SEISMIC DESIGN OF ARCHETYPE BUILDINGS

This study adopts the prescriptive design procedure for PT-CLT walls described in [13–15] and adapts it to align with design requirements in the NBCC [9]. Because the archetype building is symmetric and negligible torsion is expected, the seismic design was conducted for only one of the PT-CLT walls in the N-S direction (Fig. 3). The

https://doi.org/10.52202/080513-0493

design framework is briefly summarized here (Fig. 4). Given detailed information for each archetype (Table 1), a linear model was first established in *OpenSeesPy*, similarly to [13]. MRSA was then conducted for the linear model using the design spectrum defined in NBCC so that the peak structural responses (i.e., base shear and overturning moment) could be quantified using responses from each mode. The calculated inelastic drift ($\Delta_{inelastic}$) must be less than the NBCC 2.5% ISD limit; otherwise, iterations are needed. Next, a linear static analysis was performed using the distributed story forces determined from MRSA to calculate the panel's elastic deformation ($\Delta_{elastic}$). The rotational demand, or the maximum imposed rotation (θ_{imp}), could be then calculated as the difference between $\Delta_{elastic}$ and θ_{imp}.

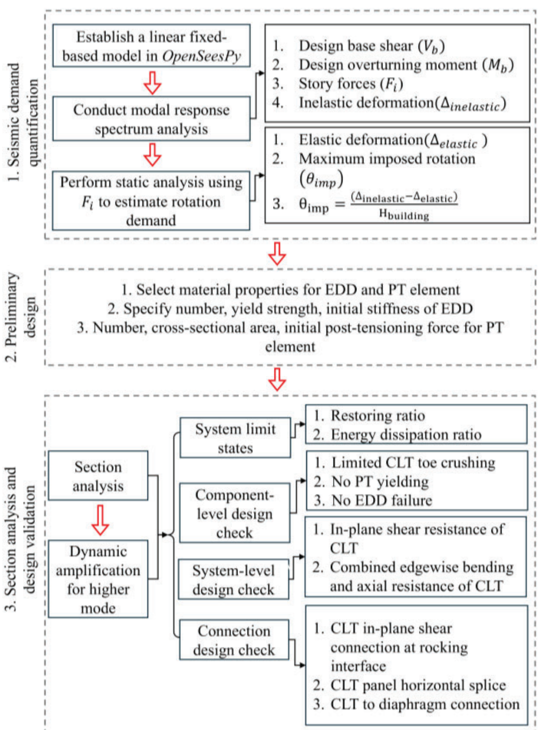

Figure 4. Prescriptive seismic design process for PT-CLT rocking wall buildings

In part 2, a preliminary design can be generated. Given a system re-centring ratio, the design overturning moment resisted by the PT element and the EDD can be initially estimated. This can lead to calculation of the initial post-tensioning forces in the PT elements and their sizing and detailing. For EDDs, an initial geometric configuration is first tentatively defined. This includes plate thickness, length, and bending diameter for UFPs or the diameter and length of the inner fuse and the outer anti-buckling system for BRAF. With material properties and geometric dimensions specified, the initial stiffness and yield strength of a single EDD can be calculated, and the required number of EDDs can be determined. The final step includes an iterative sectional analysis to verify the local and global design checks. Because existing literature has covered the sectional analysis in detail, readers are referred to Zhu et al. [8] for more information. The local design checks involve the peak component strain of CLT, PT elements, and EDDs at the θ_{imp}, whereas the global design checks assess whether the CLT wall has adequate shear and flexural resistance against demands. Note that dynamic amplification for shear force and bending moment envelopes due to higher mode effect must also be performed [13–16]. This can be particularly important, as demonstrated by past studies on self-centring rocking systems. In this study, dynamic amplification was considered using the closed-form equation developed by Wiebe and Christopoulos [16] based on the cantilever beam analogy. This method has been shown to be effective in a previous study of PT-CLT walls [6]. If the criteria for the local and global design checks are satisfied, the sectional analysis can be considered complete. Any failed criterion will lead to iteration from Part 1.

4. NUMERICAL MODELLING OF ARCHETYPES IN OPENSEESPY

4.1 MODELLING STRATEGIES

To perform nonlinear analysis, robust numerical models are required. In this study, a multi-spring modelling strategy was adopted to develop a two-dimensional models PT-CLT walls in *OpenSeesPy (*Fig. 5). The modelling approach uses a series of zero-length elements (ZLEs) at the wall-to-foundation interface to capture rocking behaviour and compressive damage at the plastic zone of the CLT panel. ZLEs can be distributed across the wall length using a *Labatto* integration method. The top of each ZLE is connected to the bottom node of the CLT panel by a *rigid link* element, whereas the bottom is fully fixed. Horizontal restraint is imposed on the ZLEs at the two extreme wall edges to prevent sliding. Based on CLT compression testing reported in [3], it was found that the *Concrete01* material model, which is a compression-only material with zero tensile strength, can effectively capture CLT yielding, post-yielding degradation, and base uplift behaviour. The concept of contact stiffness is then used to translate the CLT's stress-strain relationship into the force-deformation response of each ZLE [14]. Above the multi-spring portion, CLT panels can be assumed to be linearly elastic and modelled by *ElasticTimoshenko* beam elements. The PT elements are modelled by *corotational*

https://doi.org/10.52202/080513-0493

trusses assigned to the *Steel02* material. The top of the PT tendon is connected to the upper portion of the CLT panel using *rigid elements*. Zero-length elements with calibrated uniaxial material properties in the vertical direction are used to model EDDs, the details of which can be found in [7–8]. At the EDD location, *zero-length elements* are rigidly connected to the nodes in CLT walls at the same height to account for the offset between the walls and the EDD. In the CWC configuration, the boundary columns are pinned at the base and modelled by *elastic beam-column elements* [14]. An additional gravity-leaning column representing the gravity system is defined to capture potential P-Delta effects. The leaning column was modelled with *elastic beam-column elements* and was pinned at the foundation. Each floor node on the leaning column was rigidly connected to the floor node on the CLT wall. *Zero-length elements* with negligible rotational stiffness were defined at the junction of the floor node and its adjacent elastic columns to simulate moment release. For simplicity, Fig. 5 does not include the leaning column, but it is applied to all configurations of the numerical models.

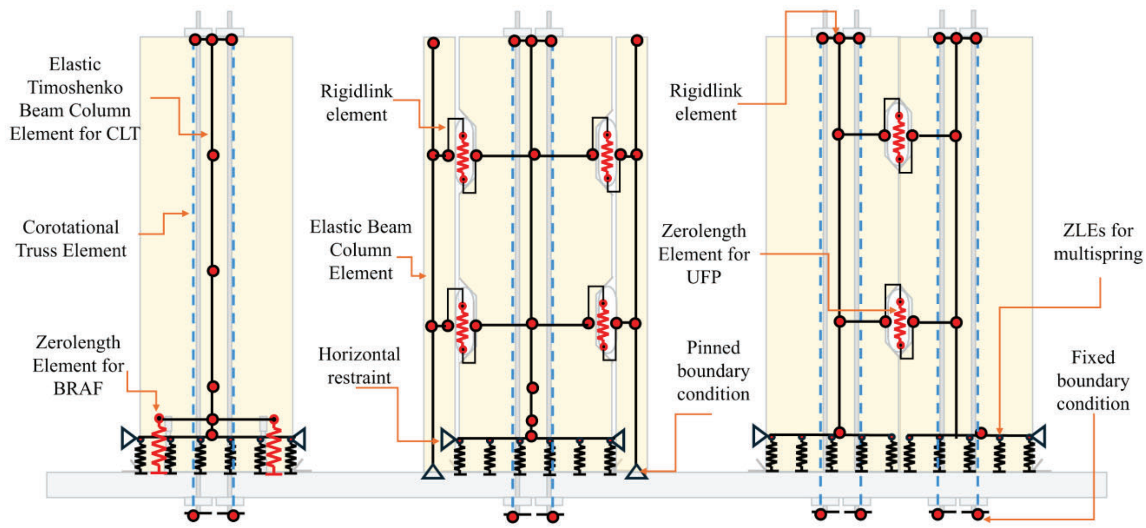

Figure 5. Schematics of multi-spring numerical models for PT-CLT rocking walls.

4.2 VALIDATION OF MODELLING STRATEGY WITH FULL-SCALE EXPERIMENTAL TESTS

To ensure the robustness of the model, building-level validation was performed with shaking table tests of the 10-story PT-CLT wall building reported by Pei et al. [4]. For more information on building design, construction details, material properties, and ground motion selection and scaling, readers are directed to Wichman [14]. A three-dimensional multi-spring numerical model was developed for the entire structure, incorporating six gravity columns, four PT rocking timber walls (two PT-CLT walls and two PT mass plywood panels (MPPs)), and eight associated boundary columns (Fig. 6a). UFPs were positioned to connect the boundary columns and the wall at the mid-height of each story. At each level, a master node was defined so that other nodes on the same floor could be constrained to it to act as a rigid diaphragm. Seismic mass reported by [14] was defined at the floor master node in two lateral and torsional directions. To better capture compressive damage at wall toes, multi-spring ZLE elements were distributed in a three-dimensional regime to capture rocking in both the in-plane and out-of-plane directions [14].

NLRHA was performed using ground motion acceleration histories obtained from shaking table tests. Time histories of floor displacements at three heights (i.e., floor levels 3, 6, and 10) of the tested structure were presented for two specific tests (ID numbers 31 and 91) and compared with the shaking table test results (Fig. 6). These tests correspond to different seismic hazard levels: a return period of 225 years (Fig. 6c), and MCE_R (Fig. 6d). Because the two PT-CLT walls were oriented in the east-west direction, the floor displacements presented in Fig. 6 represent responses that are aligned with that axis only, even though some tests involved bidirectional seismic excitation. The results showed that the model accurately predicted displacement demands in terms of both pattern and peak values across low- and high-hazard intensities. A slight underestimation was observed in Test 91, which was potentially due to the cumulative softening of the structure from previous tests and the exclusion of non-structural elements in the numerical model. Overall, the multi-spring

https://doi.org/10.52202/080513-0493

numerical modelling approach proved robust in capturing the nonlinear dynamic behaviour of PT-CLT rocking walls, making it a reliable tool for subsequent performance assessments of archetype buildings.

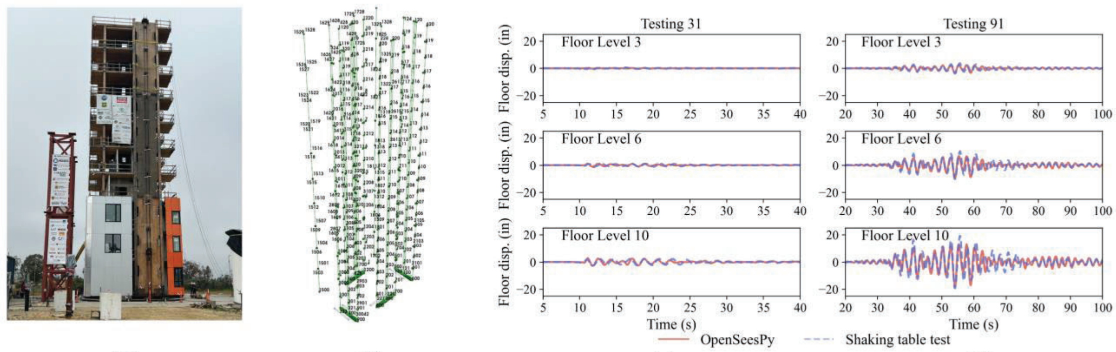

(a) (b) (c) (d)

Figure 6. Numerical model validation: (a) full-scale PT-CLT rocking wall building tested on shaking table (picture courtesy of Matiyas A. Bezabeh); (b) numerical model in OpenSeesPy; and (c-d) time-history comparison of floor displacements between OpenSeesPy and shaking table test.

5. NONLINEAR STATIC AND DYNAMIC ANALYSIS

5.1 NONLINEAR STATIC ANALYSES

Although nonlinear static analysis (NLSA) is not required in the CCMC method, in this study, we applied NLSA to validate the trial R_o factor. Each building was monotonically pushed, with load distribution corresponding to the first mode of the structure using a displacement-control integrator until 5% roof drift (a non-simulated collapse mechanism based on [4–5, 15]. Simulated collapse mechanisms applied component strain limits using the *MinMax* material in *OpenSeesPy*. A strain limit of 6% was adopted for BRAFs in the SW configuration to implicitly model low-cycle fatigue failure [7, 15]. To consider the impact of the large tensile strain of PT element, a 2% tensile strain limit was imposed [6-8]. This inherent conservatism should be recognized here because residual strength remains when the specified strain limits are reached.

Based on the pushover curves, overstrength factor can be obtained by taking the ratio between the peak shear force and the design base shear. PG overstrength was determined by averaging the overstrength of the individual archetype buildings within the PG, as shown in Fig. 7. For all the PGs, the calculated overstrength factors were greater than the trial value of $R_o = 1.5$, and this consistency was independent of structural configuration and seismic category (location). The mean values of overstrength were 2.91, 2.96, and 3.05 for SW, CWC, and CW archetypes when designed using $R_d = 4$. This result aligns well with the overstrength factor reported for PT-LVL walls in [15].

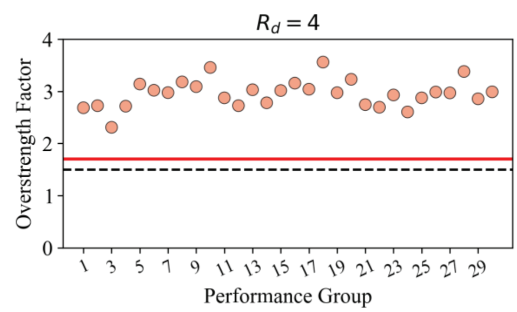

Figure 7. Performance group overstrength factor

5.2 GROUND MOTION SELECTION

To carry out NLRHA, ground motion sets for Vancouver and Montreal, as recommended by the NRCC-CRC, were adopted in this study [11]. In Vancouver, a total of 44 ground motion records were selected, consisting of 11 records from shallow crustal events, 11 from deep in-slab events, and 22 from interface events; these were scaled over period ranges of 0–1.0 s, 0–1.0 s, and 1.0–4.0 s, respectively. In addition, 32 crustal ground motions were selected for Montreal and scaled between 0–4.0 s. These scaling period ranges were provided in the report by [11] and were based on the contributions of each earthquake type to total seismic hazard [2].

5.3 NONLINEAR RESPONSE HISTORY ANALYSES

With the selected and scaled ground motions, in Step 5 of the CCMC approach (Fig. 2), NLRHA was first performed using ground motion scaled to 100% DLE level to assess seismic performance. Note that at 100%

DLE level, the peak ISD of an individual archetype should be less than 2.5%, and the ground motion leading to exceeding this limit should not be more than 10% of the total ground motion. Although a detailed tabular result is not shown due to space limitations, out of 69 designed buildings, only two SW archetypes (ID 5 and 6 in Table 1) had exceedance rates of 19% and 12% respectively, violating the 10% limit. Note that both buildings were intentionally designed to exceed current NBCC height limits for CLT buildings. Furthermore, as reported in Zhu et al. [7], SW-type buildings concentrate energy dissipation at the wall-to-foundation interface, unlike a distributed dissipation along the height of the building, as in CW or CWC. Hence, their drift-controlling capacity can be slightly undermined. Nonetheless, when examining archetypes using ground motion scaled to 200% DLE (Step 6 of CCMC) (Fig. 2), all archetypes satisfied the acceptance criteria as outlined in the method (i.e., less than 50% of ground motions leading to exceedance of 4.5% ISD).

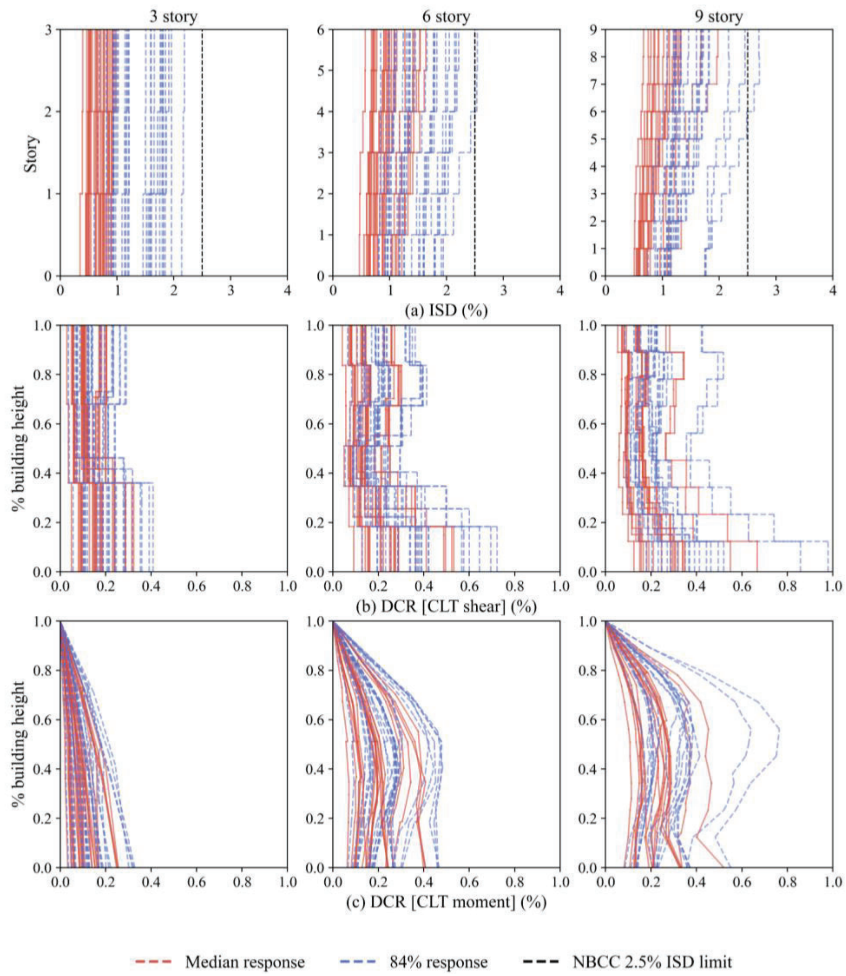

Figure 8. Median and 84% percentile structural responses under 100% DLE; (a) ISD response; (b) story shear force; (c) story overturning moment.

To better demonstrate the adequacy of the seismic performance of PT-CLT rocking walls, Figs. 8 and 9 present the structural responses of archetypes under 100% and 200% DLE respectively. The archetypes are grouped and presented based on the number of stories. For each individual building, the median and 84% percentile responses (i.e., mean plus one standard deviation) are presented. At 100% DLE, none of the buildings had a median response exceeding 2.5% ISD limit per NBCC, and only two out of 69 archetypes had 84% percentile responses marginally exceeding the limit. Consistent observations can be found in Fig. 9, where no building's median response was greater than the considered 4.5% ISD limit. During NLRHA, although limited CLT crushing is acceptable at the wall toe, the upper portion should be capacity-protected. Hence, besides global drift, the peak story force and the overturning moment were also extracted and normalized by CLT's shear and bending capacity calculated based on the Canadian CLT Handbook [17]. The results are

https://doi.org/10.52202/080513-0493

presented in Figs. 8 and 9. At both DLE levels, the median peak demand capacity ratios (DRCs) for all archetypes were less than 1 (for both CLT edgewise shear and bending), highlighting the satisfactory seismic design and performance.

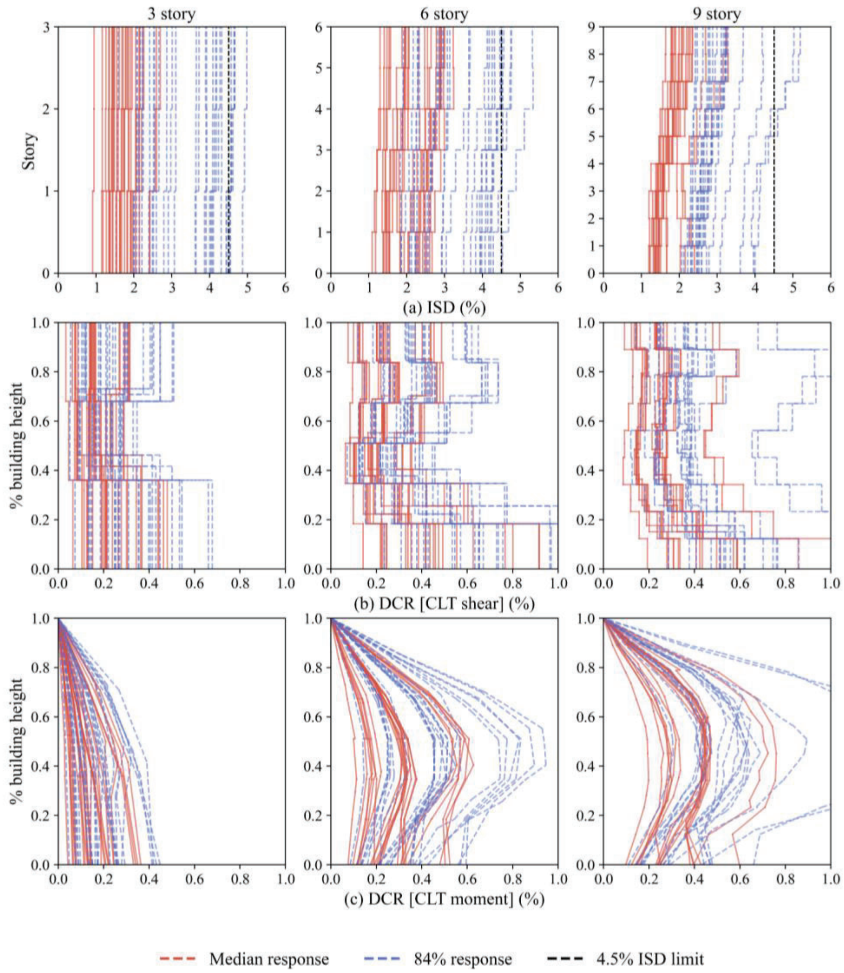

Figure 9. Median and 84% percentile structural responses under 200% DLE: (a) ISD response; (b) story shear force; (c) story overturning moment.

8. SUMMARY AND CONCLUSION

With over two decades of research on the seismic performance of PT-CLT walls, efforts are ongoing to codify the system into major building codes and design standards. For practical adoption of this SFRS in Canada, R_o and R_d factors are essential for seismic design. However, these factors are currently not available in the latest editions of the NBCC. This study evaluated the R_d and R_o factors for PT-CLT rocking walls with EDDs following the CCMC procedure and considering the extensive damage performance objective outlined in NBCC. An R_o of 1.5 and an R_d factor of 4 were initially considered. To reflect potential variability in building geometry, system configuration, and seismic hazards, 69 archetype buildings were designed in this study. A robust multi-spring numerical modelling strategy in *OpenSeesPy* was validated with full-scale shaking table tests and then used to model all archetype buildings. Nonlinear static analysis was carried out and demonstrated that system overstrength factors were consistently higher than the proposed $R_o = 1.5$. Following the CCMC procedure, NLRHA was performed using site-specific ground motions scaled to 100% and 200% DLEs. The archetypes were then evaluated against CCMC's acceptance criteria. The results indicated that the adopted prescriptive seismic design with $R_d R_o = 6$ ensures satisfactory building performance, with peak ISD remaining below the NBCC limit and CLT panels adequately capacity protected. Future work should aim to develop a seismic design guideline to complement the *CSA O86 Engineering Design in Wood* considering the R_d and R_o factors from this study.

REFERENCES

[1] Karacabeyli, E., & Lum, C. (Eds.). (2022). *Technical guide for the design and construction of tall wood buildings in Canada* (2nd ed.), FPInnovations, Pointe-Claire, QC, Canada.

[2] Yang, T. Y., Lepine-Lacroix, S., Guerrero, J. A. R., McFadden, J. B. W., & Al-Janabi, M. A. Q. (2022). Seismic performance evaluation of innovative balloon-type CLT rocking shear walls. *Resilient Cities and Structures, 1*(1), 44–52. https://doi.org/10.1016/j.rcns.2022.03.004

[3] Chen, Z., Popovski, M., & Iqbal, A. (2020). Structural performance of post-tensioned CLT shear walls with energy dissipators. *Journal of Structural Engineering, 146*(3), 04020035. https://doi.org/10.1061/(ASCE)ST.1943-541X.0002569

[4] Pei, S., Ryan, K. L., Berman, J. W., Van De Lindt, J. W., Pryor, S., Huang, D., Wichman, S., Busch, A., Roser, W., Wynn, S. L., Ji, Y., Hutchinson, T., Sorosh, S., Zimmerman, R. B., & Dolan, J. D. (2024). Shake-table testing of a full-scale 10-story resilient mass timber building. *Journal of Structural Engineering, 150*(2), 04024183. https://doi.org/10.1061/JSENDH.STENG-13752

[5] Pei, S., Van De Lindt, J. W., Barbosa, A. R., Berman, J. W., McDonnell, E., Dolan, J. D., Blomgren, H.-E., Zimmerman, R. B., Huang, D., & Wichman, S. (2019). Experimental seismic response of a resilient 2-story mass-timber building with post-tensioned rocking walls. *Journal of Structural Engineering, 145*(11), 04019120. https://doi.org/10.1061/(ASCE)ST.1943-541X.0002382

[6] Kovacs, M. A., & Wiebe, L. (2019). Controlled rocking CLT walls for buildings in regions of moderate seismicity: Design procedure and numerical collapse assessment. *Journal of Earthquake Engineering, 23*(5), 750–770. https://doi.org/10.1080/13632469.2017.1326421

[7] Zhu, H., Bezabeh, M., Iqbal, A., Popovski, M., & Chen, Z. (2024). Seismic performance assessment of post-tensioned CLT shear wall buildings with buckling-restrained axial fuses. *Canadian Journal of Civil Engineering.* Advance online publication. https://doi.org/10.1139/cjce-2023-0448

[8] Zhu, H., Bezabeh, M. A., Iqbal, A., Popovski, M., & Chen, Z. (2025). Seismic design and performance evaluation of post-tensioned CLT shear walls with coupling U-shaped flexural plates in Canada. *Earthquake Spectra.* Advance online publication. https://doi.org/10.1177/87552930251316263

[9] National Research Council of Canada (NRCC). (2020). *National Building Code of Canada 2020*. Canadian Commission on Building and Fire Codes, Ottawa, Canada.

[10] Federal Emergency Management Agency (FEMA). (2009). *Quantification of building seismic performance factors* (FEMA P-695). Applied Technology Council.

[11] Fazileh, F., Fathi-Fazl, R., & Huang, X. (2023). *Performance-based unified procedure for determination of seismic force modification factors Rd, R_o in NBC*. National Research Council of Canada, Construction Research Centre. https://doi.org/10.4224/40003049

[12] DeVall, R., Popovski, M., & McFadden, J. B. W. (2021). *Technical guide for evaluation of seismic force resisting systems and their force modification factors for use in the National Building Code of Canada with concepts illustrated using a cantilevered wood CLT shear wall example* (Version 3, 38 p.). National Research Council of Canada. https://doi.org/10.4224/40002658

[13] Busch, A., Zimmerman, R. B., Pei, S., McDonnell, E., Line, P., & Huang, D. (2022). Prescriptive seismic design procedure for post-tensioned mass timber rocking walls. *Journal of Structural Engineering, 148*(12), 04021289. https://doi.org/10.1061/(ASCE)ST.1943-541X.0003240

[14] Wichman, S. (2023). *Seismic behaviour of tall rocking mass timber walls* (Doctoral dissertation). University of Washington.

[15] Sarti, F., Palermo, A., Pampanin, S., & Berman, J. (2017). Determination of the seismic performance factors for post-tensioned rocking timber wall systems. *Earthquake Engineering & Structural Dynamics, 46*(2), 181–200. https://doi.org/10.1002/eqe.2784

[16] Wiebe, L., & Christopoulos, C. (2015). A cantilever beam analogy for quantifying higher mode effects in multistorey buildings. *Earthquake Engineering & Structural Dynamics, 44*(11), 1697–1716. https://doi.org/10.1002/eqe.2549

[17] Karacabeyli, E., & Gagnon, S. (Eds.) (2019) *Canadian CLT Handbook* (2nd ed.), : FPInnovations, Pointe-Claire, QC, Canada.

https://doi.org/10.52202/080513-0493